NANO LETTERS

2004
Vol. 4, No. 1
153−158

Resonant Field Enhancements from Metal Nanoparticle Arrays

Dentcho A. Genov,[†] Andrey K. Sarychev,[†] Vladimir M. Shalaev,[†] and Alexander Wei*,[‡]

Departments of Chemistry and Electrical and Computer Engineering, Purdue University, West Lafayette, Indiana 47907

Received June 5, 2003; Revised Manuscript Received November 17, 2003

ABSTRACT

Theoretical and semiempirical studies of two-dimensional (2D) metal nanoparticle arrays under periodic boundary conditions yield quantitative estimates of their electromagnetic (EM) field factors, revealing a critical relationship between particle size and interparticle spacing. A new theory based on the RLC circuit analogy has been developed to produce analytical values for EM field enhancements within the arrays. Numerical and analytical calculations suggest that the average EM enhancements for Raman scattering ($\bar{G}$) can approach 2×10^{11} for Ag nanodisks (5×10^{10} for Au) and 2×10^{9} for Ag nanosphere arrays (5×10^{8} for Au). Radiative losses related to retardation or damping effects are less critical to the EM field enhancements from periodic arrays compared to that from other nanostructured metal substrates. These findings suggest a straightforward approach for engineering nanostructured arrays with direct application toward surface-enhanced Raman scattering (SERS).

Nanostructured metal−dielectric interfaces often exhibit enhanced optical phenomena at visible and near-infrared (NIR) frequencies via excitation of surface plasmon modes.[1,2] The enticing possibilities of engineering such properties for applications in photonics and chemical sensing have led to a resurgence of activity in the design of plasmonic materials with subwavelength dimensions.[3] Enhanced electromagnetic (EM) field effects can be generated either in a broad spectral range, as is the case for disordered metal−dielectric composites,[2,4] or at select frequencies from periodically ordered metal nanostructures. Periodicity plays a key role in tuning the optical response of the latter, and has been documented in experimental and theoretical investigations of plasmon-enhanced effects such as surface-enhanced Raman scattering (SERS),[5−7] extraordinary optical transmission,[8−10] and robust photonic band gaps at visible and NIR wavelengths.[11−13]

SERS has attracted widespread attention because of its demonstrated potential for single-molecule spectroscopy and chemical sensing with high information content.[14−16] The rational design of optimized SERS substrates remains a challenging goal, despite extensive efforts to elucidate the physical basis of signal enhancement. Several theoretical studies have described highly localized EM fields at the junction of metal nanostructures,[7,17−19] with local EM enhancement factors $G_{loc} = |E_{loc}(\lambda)/E_0(\lambda)|^4$ as high as 10^{11}−10^{12} for a two-particle system.[20] However, less attention has been paid to the average EM enhancement factors ($\bar{G} = \langle G_{loc} \rangle$), which has greater relevance for the design and optimization of SERS-based chemical sensors. In this regard, García-Vidal and Pendry have provided electrodynamics calculations on periodic nanostructured metal films with $\bar{G}$ values on the order of 10^6, a level of activity commonly observed in many experimental systems.[7]

Here we provide numerical calculations and a simple analytical theory for calculating EM field enhancements in two-dimensional (2D) arrays of metal nanoparticles embedded in a dielectric medium. The numerical simulations and analytical values are in good agreement and yield $\bar{G}$ values as high as 2×10^{11} for arrays of cylindrical Ag nanodisks and 5×10^{10} for arrays of Au nanodisks. Analytical values can also be obtained for 2D arrays of metal nanospheres, yielding $\bar{G}$ values on the order of 2×10^9 and 5×10^8 for Ag and Au nanoparticles, respectively. These activities, which are up to several orders of magnitude greater than those of aperiodic metal−dielectric composites or roughened metal surfaces, are independent of morphology-dependent resonances such as those responsible for microcavity-enhanced SERS.[21] The enhancements of the nanostructured arrays are strongly dependent on the ratio of particle diameter to interparticle spacing, which determines both the intensity of local field factors and the available cross-sectional area for sampling chemical and biomolecular analytes. Our models illustrate how the interplay between field enhancement and interparticle spacing can impact the design of array-based SERS sensors for trace chemical analysis.

Numerical calculations were first performed on 2D arrays of cylindrical oblate disks with high aspect ratio and diameter

* Corresponding author. E-mail: alexwei@purdue.edu
[†] Department of Electrical and Computer Engineering.
[‡] Department of Chemistry.

10.1021/nl0343710 CCC: $27.50
Published on Web 12/09/2003

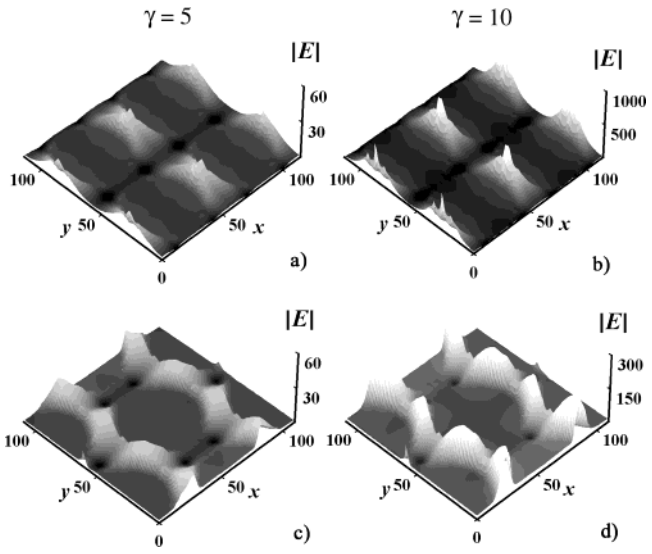

Figure 1. Cross-sectional view of local EM field factors produced by *p*-polarized light ($l = 647$ nm, $\boldsymbol{E}_0 = \boldsymbol{E}_x$) within periodic 2D arrays of Au nanodisks embedded in a low-dielectric medium ($\epsilon_d = 1.5$). Two different lattice geometries are shown: (a, b) 2D square lattice; (c, d) 2D hexagonal lattice. Two different diameter−spacing ratios are shown: (a, c) $\gamma = 5$; (b, d) $\gamma = 10$. Note the change in scale for $|E_{loc}(\mathbf{r})/E_0|$ for arrays with different values of γ. Discretization was performed using a 120 × 120 square lattice.

$d \ll \lambda$, arranged in square or hexagonal lattices in a dielectric medium ϵ_d using periodic boundary conditions (see Figure 1).[22] Such arrays can be approximated as planar systems for the purpose of estimating local field factors.[2] Here we apply the current conservation law, which can be expressed in terms of a local potential $\varphi(\mathbf{r})$

$$\nabla\cdot[\sigma(\mathbf{r})(-\nabla\varphi(\mathbf{r}) + \boldsymbol{E}_0)] = 0 \qquad (1)$$

where $\boldsymbol{E}_0$ is the incident electric field, $\sigma(\mathbf{r}) = -i\omega\epsilon_m/4\pi$ is the local conductivity, and $\epsilon_m = \epsilon'_m + i\epsilon''_m$ is the complex dielectric function of the metal. Describing the continuity equation in these terms allows the collective plasmon response to be determined under quasistatic conditions in a scale-invariant manner.[2] In addition, $E_{loc}(\mathbf{r})/E_0$ can be calculated as a continuous function of packing density, described by a single geometric parameter $\gamma = d/\delta$, where d is the distance between the particles at the point of closest approach. The parameter γ is fundamentally important, because the resonance condition can be derived directly from Poisson's equation to yield the simple relationship $\epsilon'_m \approx -\gamma\epsilon_d$.

It is important to note that the quasistatic approximation is valid for nanoparticle arrays with periodicities below the diffraction limit ($\lambda/2$). Radiative loss from elastic (Rayleigh) scattering is negligible, and losses due to retardation effects (a function of the finite skin depth of nanoparticles larger than 30 nm) can be accounted for by a first-order correction (see below).[2] Furthermore, for a 2D nanoparticle array where $\gamma \gg 1$, the spatial localizations of the EM resonances between particles are well within the quasistatic limit.

Discretization of eq 1 on a square-mesh lattice under periodic boundary conditions yielded L^2 equations ($L = 120$), which were solved by the exact block elimination approach.[23] This method provides solutions for site potentials corresponding to $E_{loc}(\mathbf{r})/E_0$ in L^4 operations, an enormous savings in computing time compared with the L^6 operations required by Gaussian elimination methods.[24] $\bar{G}$ is obtained simply as the mean value of $G_{loc} = |E_{loc}(\mathbf{r})/E_0|^4$ within a unit cell of the periodic lattice. We note that these calculations are equally valid for periodic arrays of nanowires at constant depth as for oblate metal nanodisks with high aspect ratio, whose electric fields and currents are confined to the plane of the system.[2]

The intensities of the local and average EM field enhancements depend greatly on both incident wavelength and diameter−spacing ratio (see Figures 1 and 2 for G_{loc} and $\bar{G}$ of Au nanodisk arrays at different values of γ). Au nanodisk arrays with large diameter−spacing ratios ($\gamma \geq 30$) can produce G_{loc} values as high as 10^{10}, whereas Ag nanodisk arrays can produce G_{loc} values as high as 10^{12}. These optical gains are the product of wavelength-selective resonant modes within the periodically ordered arrays (see below).[22] With respect to the average EM enhancements, $\bar{G}$ can be described as a resonance band whose width increases with γ. Arrays with large γ can produce high $\bar{G}$ over a greater range of excitation wavelengths, which has important practical ramifications for SERS.

The highest $\bar{G}$ values ($\bar{G}^{max}$) can be several orders of magnitude greater than that generated by a random metal-dielectric film at the percolation threshold ($p = p_c$), as well as those produced by periodic gratings whose plasmonic responses are at the saturation limit for continuous metal films (see Figure 2).[7] In contrast, average field enhancements outside of the resonance band are much lower than those generated by broadband amplifiers such as disordered metal-dielectric films. Introducing disorder into the 2D arrays also substantially decreases $\bar{G}$, indicating that long-range order is an important factor for generating high local EM resonant enhancements, which in turn provide the greatest contribution to $\bar{G}$.

The intensities of the local field enhancements that comprise $\bar{G}$ are also dependent on their spatial relationship within the nanoparticle array, and also in their relationship with the polarization of the incident wavevector. In our calculations, values for E_{loc} were obtained at fixed diameter-spacing ratios with the incident light polarized along the *x*-axis, such that the local EM enhancements are greatest at sites between particles along the direction of polarization (see Figure 1 for $\gamma = 5$ and 10). However, a change in the polarization angle produces large shifts in the positions and intensities of the maximum local field factors, with a small reduction in the average EM enhancements (see Figure 3). For example, $\bar{G}$ values produced by square-lattice 2D arrays decrease by a factor of 2 when θ changes from 0° to 45°. The polarization angle is likely to be an important parameter for single-molecule SERS and related spectroscopies, in which the analytes of interest are thought to be localized between particles.[14,15,25] In this scenario, the Raman signals can be maximized by adjusting θ until the highest local fields are coincident with the exact position of the molecule.

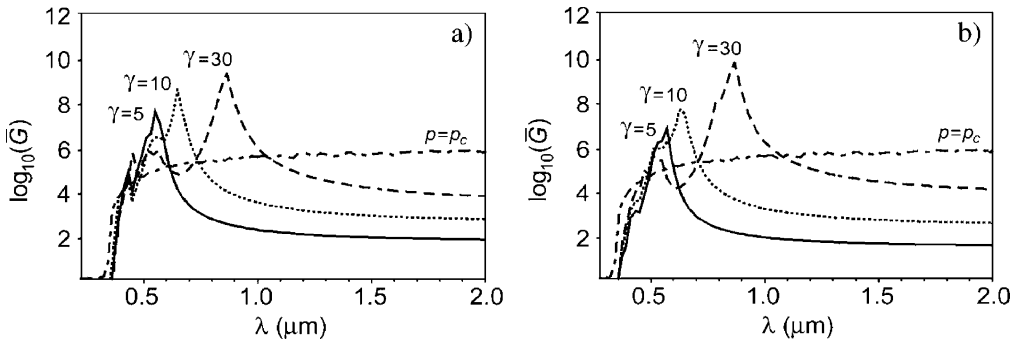

Figure 2. Average EM enhancements ($\bar{G}$) from 2D arrays of Au nanodisks as a function of incident wavelength (λ) at fixed particle diameter−spacing ratios (γ = 5, 10, and 30): (a) 2D square lattice; (b) 2D hexagonal lattice. A plot of $\bar{G}$ from random metal−dielectric films at the percolation threshold ($p = p_c$) is included for comparison.

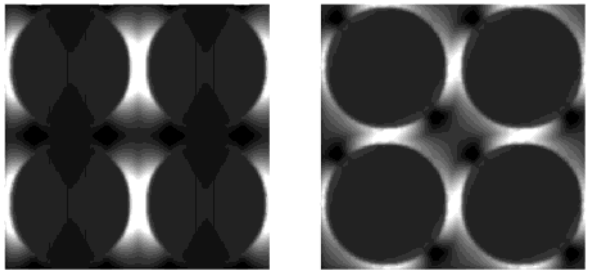

Figure 3. Local EM field distributions and intensities at different polarization angles. Left, $\theta = 0°$ ($E_0 = E_x$); Right, $\theta = 45°$.

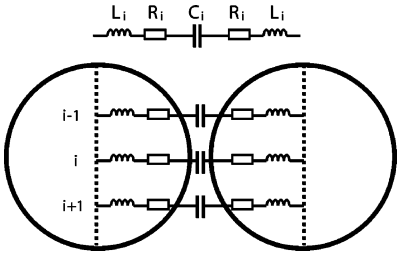

Figure 4. Frequency-dependent plasmon response depicted as an array of RLC circuits.

To confirm the validity of the numerical calculations under quasistatic conditions, we have developed an analytical approach for estimating $\bar{G}$. The EM coupling between metal nanoparticles can be conceptualized as arrays of RLC circuits across the interparticle gap, with each element *i* representing a resonance defined by local spacing δ_i (see Figure 4).[2] The negative permittivity of the metal ($\epsilon'_m < 0$) and the dielectric ϵ_d are represented respectively by inductance $R-L$ and capacitance C. The RLC model suggests that the collective plasmon resonances of the 2D nanoparticle arrays should shift strongly toward lower frequencies (high LC) with increasing γ, in accord with our numerical simulations and recent calculations involving metal nanoparticle dimers (see Figure 2).[20] In addition, the model is consonant with the broadening of the plasmon bandwidths that occurs with red-shifting, which reflects a greater degeneracy of EM states at high γ due to the effectively greater radius of curvature at the interface between particles.

The RLC model provides a theoretical framework for describing changes in EM Raman enhancement as a function of γ and ϵ_m. Under low-loss conditions the dielectric function can be expressed as $\epsilon_m = \epsilon'_m(1 - i\kappa)$, where $\epsilon'_m < 0$ and loss factor $\kappa \ll 1$. If $\gamma \gg 1$ and the surrounding dielectric ϵ_d is taken into account, one can derive an expression for an effective dielectric function ϵ_{eff}

$$\epsilon_{eff} \cong |\epsilon'_m|\left(\frac{\pi}{\sqrt{2\kappa(\Delta - i)(W + 1)}} - \frac{(1 + \pi/2)}{(W + 1)}\right) \qquad (2)$$

where parameters $W = |\epsilon'_m|/\epsilon_d$ and $\Delta = (W/\gamma - 1)/\kappa$ (see Supporting Information for more details). This composite dielectric function reaches a maximum when $\Delta \to 0$, so that $\epsilon_{eff}^{max} \cong |\epsilon'_m|(1 + i)\pi/\sqrt{4\kappa(W + 1)}$. If $\Delta > 1$, ϵ_{eff} is mostly real and larger than ϵ_d, such that the array response is dominated by interparticle capacitance (C). If $\Delta < 0$, the imaginary part of ϵ_{eff} prevails, resulting in large losses and subsequently large fluctuations in local field. It is worth noting that the effective absorption of the metal−dielectric composite, ϵ''_{eff}, is proportional to $\sqrt{|\epsilon_m|/\kappa}$ near resonance, which increases as κ goes to zero. A high effective absorption is necessary to produce giant fluctuations in the local fields between particles and determines the capacity of the 2D arrays to accumulate and release EM energy.

The EM enhancement factor $\bar{G}$ (averaged over the unit cell, minus metal particles) can now be expressed analytically as

$$\bar{G} \cong \frac{\pi(W + 1)^{7/2}}{2((4 - \pi)W + 4)\kappa^{7/2}} \times \sqrt{\frac{4\Delta^2 + 9}{(\Delta^2 + 1)^{3/2}} - \frac{\Delta(4\Delta^4 + 15\Delta^2 + 15)}{(\Delta^2 + 1)^3}} \qquad (3)$$

(see Supporting Information for more details). The maximum EM enhancement $\bar{G}^{max}$ is also achieved when $\Delta \to 0$; if a Drude free-electron response is assumed in which $\epsilon'_m(\omega) = 1 - (\omega_p/\omega)^2$ and $\kappa = \omega_\tau/\omega$, with plasma frequency $\omega_p \gg \omega$ and relaxation frequency $\omega_\tau \ll \omega$, parameter W can be approximated as $(\omega_p/\omega)^2\epsilon_d^{-1}$ and $\bar{G}^{max}$ can then be estimated as

$$\bar{G}^{max} \cong \pi(\omega_p/\sqrt{\epsilon_d})^5\omega_\tau^{-7/2}\omega_{res}^{-3/2} \qquad (4)$$

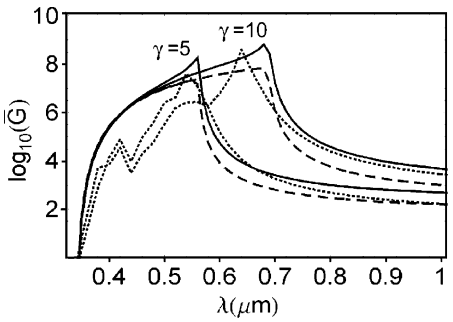

Figure 5. Analytical solutions of average EM enhancements ($\bar{G}$) as a function of λ for 2D square-lattice arrays of Au nanodisks and nanospheres (solid and dashed curves, respectively), calculated for $\gamma = 5$ and 10. The corresponding numerical solution for the 2D nanodisk array (dotted curve) is included for comparison.

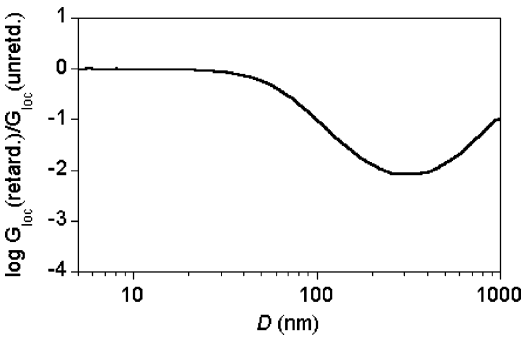

Figure 6. Ratio of G_{loc} values (located midway between gold nanodisks) calculated with and without retardation effects as a function of lattice period D. Nanoparticles are arranged in a square-lattice array with $\gamma = 30$ and incident wavelength $\lambda = 1$ μm.

in which the resonance frequency is defined as $\omega_{res} \approx \omega_p(\gamma\epsilon_d)^{-1/2}$. For the case of Au nanodisk arrays, we use $\omega_p = 9.3$ eV and $\omega_\tau = 0.03$ eV[26] to obtain an approximate $\bar{G}^{max}$ value of $5 \times 10^{10}\epsilon_d^{-5/2}\lambda_{res}^{3/2}$, where $\lambda_{res} = 2\pi c/\omega_{res}$ is the resonance wavelength expressed in μm. For the case of Ag ($\omega_p = 9.1$ eV, $\omega_\tau = 0.021$ eV[26]) we obtain a $\bar{G}^{max}$ value of $2 \times 10^{11}\epsilon_d^{-5/2}\lambda_{res}^{3/2}$, which is four times larger than that of gold.

The analytical expressions derived from the RLC model are in excellent agreement with the numerical calculations of $\bar{G}$ for the 2D nanowire arrays at different values of γ (see Figure 5). It is particularly noteworthy that the analytical $\bar{G}^{max}$ values are essentially identical with those obtained by numerical calculations under quasistatic conditions. It should be noted, however, that the numerical calculations exhibit additional maxima at shorter wavelengths that are not present in the analytical solutions. These peaks are likely related to artifacts resulting from the discretization procedure.

For periodic 2D arrays of metal nanospheres, the analytical expression for the effective dielectric function is rather different from eq 2:

$$\epsilon_{eff,sph} \cong 2\epsilon_d\left[\left(1 + \frac{\kappa\Delta}{W+1}\right)\log\left(\frac{W+1}{\kappa(\Delta - i)}\right) - 1\right] \quad (5)$$

As in the case of metal nanodisk arrays, the imaginary part of ϵ_{eff} prevails when $\Delta < 0$, producing large fluctuations in local field. The average EM enhancement between nanospheres is then expressed as

$$\bar{G}_{sph} \cong \frac{3(W+1)^3}{(W+3)\kappa^3}\left[\frac{\pi}{2} - \frac{\Delta}{1+(\Delta+\kappa)^2} - \tan^{-1}(\Delta+\kappa)\right] \quad (6)$$

where $\bar{G}_{sph}$ is further averaged in the z-dimension between $+d/2$ and $-d/2$. Assuming a Drude free-electron response, the maximum EM enhancement $\bar{G}_{sph}^{max}$ can be estimated as

$$\bar{G}_{sph}^{max} \cong (3\pi/2)\omega_p^4\epsilon_d^{-2}\omega_\tau^{-3}\omega_{res}^{-1} \quad (7)$$

in which the resonance frequency is again defined as $\omega_{res} \approx \omega_p(\gamma\epsilon_d)^{-1/2}$. Substituting in the same optical constants as before, we find that the $\bar{G}_{sph}^{max}$ values for Ag and Au nanosphere arrays are approximately $2 \times 10^9\epsilon_d^{-2}\lambda_{res}$ and $5 \times 10^8\epsilon_d^{-2}\lambda_{res}$, respectively. The nearly two order-of-magnitude difference between eqs 4 and 7 can be ascribed to the change in unit particle geometry. In the case of the 2D disk arrays, plasmonic contributions to the local EM field strength are constant with respect to depth, whereas in the case of the 2D nanosphere array the field strength rapidly decreases with distance from the particle surfaces. Nevertheless, the resonance behaviors of the two systems are entirely analogous with respect to γ and ϵ_{eff}.

The analyses thus far have been performed using quasistatic approximations in which retardation effects are assumed to be negligible. However, such effects may become significant when the particle size or lattice constant is no longer small compared with the incident wavelength. Here we estimate the extent to which retardation effects influence G as a function of lattice periodicity D, for a given diameter−spacing ratio ($\gamma = 30$; see Figure 6). Local field factors were calculated by solving the coupled-dipole equations both with and without retarded potentials for very large square-lattice arrays of Au nanodisks ($N \sim 10^6$; see Supporting Information for more details).[27] A comparison of these factors reveals no effects of retardation on G_{loc} for periodicities up to 40 nm, after which a gradual decrease ensues. Even so, the retarded G values remain relatively high, indicating that periodic order can significantly reduce radiation losses in arrays of particles which otherwise experience significant retardation effects.

Finally, we collate the theoretical relationship between EM enhancement and periodic structure with some recent experimental SERS measurements, taken from hexagonally close-packed 2D arrays of colloidal gold nanoparticles whose diameter−spacing ratios range from approximately 15−100 (see Figure 7).[5] The empirical Raman signal enhancements (G_{SERS}) are amplified by local EM field factors and are proportional to $\bar{G}$ with the modification that $G_{SERS} = |E(\lambda)/E_0(\lambda)|^2|E(\lambda')/E_0(\lambda')|^2$, where λ and λ' are the incident and Stokes-shifted wavelengths, respectively.[2,28] In our theoretical considerations we take into account the skin effect by renormalizing the dielectric permittivity (see Supporting Information for more details). We also take into account the loss of incident field due to reflection and absorption at the

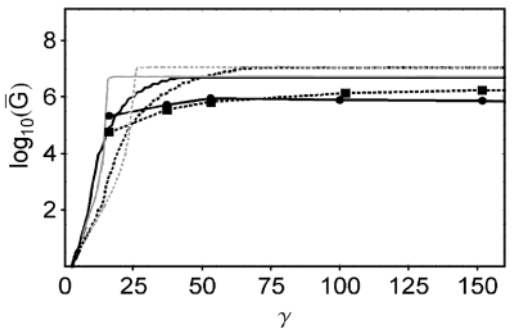

Figure 7. Average EM enhancements calculated with first-order correction ($\bar{G}'$) for 2D hexagonal arrays of Au nanospheres at $\lambda =$ 647 nm (solid curves) and 785 nm (dotted curves), in comparison with the corresponding G_{SERS} values (circles and squares, respectively). Retardation effects due to finite skin depth are taken into account in the analytical theory. $\bar{G}'$ values for 2D arrays with exact γ (in gray) are superimposed over those in which a variance of 30% has been assumed (in black).

air−metal interface by introducing a first-order correction to the enhancement factor $\bar{G}' = T^2 G_{av}$, where T is the transmission coefficient ($T \sim 0.25$ based on experimental extinction measurements).[5] Even so, the comparison between experiment and theory remains semiquantitative, as the empirical G_{SERS} values also depend on several other factors such as chemical "first-layer" effects and the efficiency of the collection optics.

Analytical EM enhancement values were calculated for 2D arrays of Au nanospheres at fixed incident wavelengths ($\lambda_{ex} =$ 647, 785 nm), in which local order was assumed. Values for $\bar{G}'$ were obtained as means of distributions about a given value of γ using a 30% coefficient of variance to account for the limited precision of measurement.[5] These enhancements are in fact very similar to $\bar{G}'$ values derived for crystalline 2D arrays with precisely defined spacings, particularly as γ becomes large (see Figure 7). The comparison of $\bar{G}'$ with empirical G_{SERS} values reveals similar trends with respect to γ, demonstrating good correlation between experiment and theory.

Two additional observations are worthy of discussion. First, for a given incident wavelength, $\bar{G}$ is essentially equivalent to $\bar{G}^{max}$ when γ is above a threshold value. This is a consequence of the tradeoff between G_{loc}, whose maximum intensities increase rapidly with γ, and the total available field volume which decreases with γ. The wide range of diameter−spacing ratios that can provide $\bar{G}^{max}$ is of great practical benefit for designing 2D nanoparticle arrays as SERS-based chemical sensors. However, it is also necessary to consider geometrical requirements for accessing high-field regions, so that analyte molecules can be rapidly detected. Highly localized EM field enhancements have a lower probability of detecting exogenous analytes than those which are diffused over a larger cross-sectional area; therefore, the optimal diameter−spacing ratio should be the threshold value of γ which produces $\bar{G}^{max}$ with the greatest possible sampling volume.

Second, both theoretical and empirical $\bar{G}$ values of the 2D nanoparticle arrays remain approximately constant as γ increases with respect to the wavelength, i.e., with increasing $d/\lambda \cdot \delta$, in contrast to that calculated and observed in isolated nanospheres for which G decreases as d/λ becomes large.[29−31] This again indicates that size-dependent radiative damping, which is known to degrade field factors from isolated metal nanoparticles as an approximate function of particle volume, does not have a strong effect on the SERS activities of the 2D nanoparticle arrays. The modest effect of particle size on G_{SERS} from the experimental system further supports our notion that damping and retardation effects are minimized when the local EM fields are spatially confined to volumes within the quasistatic limit.

Acknowledgment. The authors gratefully acknowledge the National Science Foundation (BES-0228143, CHE-0243496, ECS-0210445, DMR-0121814), ARO/Temeku Technologies, Inc. (DAAD19-00-R-0010, DAAD19-01-1-0682), NASA (NCC-1-01049), and the Indiana Proteomics Consortium for financial support. This work is in association with the Center for Sensing Science and Technology and the Birck Nanotechnology Center at Purdue University.

Supporting Information Available: Additional details and explanations for the derivation of eqs 2−7, and corrections for retardation effects. This material is available free of charge via the Internet at http://pubs.acs.org.

References

(1) Raether, H. *Surface Plasmons on Smooth and Rough Surfaces and on Gratings*; Springer: Berlin, 1988.
(2) Sarychev, A. K.; Shalaev, V. M. *Phys. Rep.* **2000**, *335*, 275−371. (b) Shalaev, V. M. *Nonlinear Optics of Random Media: Fractal Composites and Metal-Dielectric Films*; Springer: Heidelberg, 2000.
(3) Wei, A. In *Nanoparticles: Scaffolds and Building Blocks*; Rotello, V. M., Ed.; Kluwer Academic: New York, 2003.
(4) Stockman, M. I.; Shalaev, V. M.; Moskovits, M.; Botet, R.; George, T. F. *Phys. Rev. B* **1992**, *46*, 2821−30. (b) Grésillon, S.; Aigouy, L.; Boccara, A. C.; Rivoal, J. C.; Quelin, X.; Desmarest, C.; Gadenne, P.; Shubin, V. A.; Sarychev, A. K.; Shalaev, V. M. *Phys. Rev. Lett.* **1999**, *82*, 4520−23.
(5) Wei, A.; Kim, B.; Sadtler, B.; Tripp, S. L. *ChemPhysChem* **2001**, *2*, 743−45. (b) Kim, B.; Tripp, S. L.; Wei, A. *J. Am. Chem. Soc.* **2001**, *123*, 7955−56.
(6) Wirgin, A.; López-Ríos, T. *Optics Commun.* **1984**, *48*, 416−20.
(7) Garcia-Vidal, F. J.; Pendry, J. B. *Phys. Rev. Lett.* **1996**, *77*, 1163−66.
(8) Ebbesen, T. W.; Lezec, H. J.; Ghaemi, H. F.; Thio, T.; Wolff, P. A. *Nature* **1998**, *391*, 667−69. (b) Ghaemi, H. F.; Thio, T.; Grupp, D. E.; Ebbesen, T. W.; Lezec, H. J. *Phys. Rev. B* **1998**, *58*, 6779−82.
(9) Porto, J. A.; Garcia-Vidal, F. J.; Pendry, J. B. *Phys. Rev. Lett.* **1999**, *83*, 2845−48.
(10) Sarychev, A. K.; Podolskiy, V. A.; Dykhne, A. M.; Shalaev, V. M. *IEEE J. Quantum Elect.* **2002**, *8*, 956−63. (b) Dykhne, A. M.; Sarychev, A. K.; Shalaev, V. M. *Phys. Rev. B* **2003**, *67*, 195402.
(11) Moroz, A. *Phys. Rev. Lett.* **1999**, *83*, 5274−77.
(12) Zhang, W. Y.; Lei, X. Y.; Wang, Z. L.; Zheng, D. G.; Tam, W. Y.; Chan, C. T.; Sheng, P. *Phys. Rev. Lett.* **2000**, *84*, 2853−56.
(13) Podolskiy, V. A.; Sarychev, A. K.; Shalaev, V. M. *Opt. Express.* **2003**, *11*, 735−45.
(14) Kneipp, K.; Kneipp, H.; Itzkan, I.; Dasari, R. R.; Feld, M. S. *Chem. Rev.* **1999**, *99*, 2957−75.
(15) Xu, H. X.; Bjerneld, E. J.; Kall, M.; Borjesson, L. *Phys. Rev. Lett.* **1999**, *83*, 4357−60.
(16) Vo-Dinh, T. *Trends Anal. Chem.* **1998**, *17*, 557−82.
(17) Aravind, P. K.; Nitzan, A.; Metiu, H. *Surf. Sci.* **1981**, *110*, 189−204.
(18) Liver, N.; Nitzan, A.; Gersten, J. I. *Chem. Phys. Lett.* **1984**, *111*, 449−54.

(19) Jensen, T.; Kelly, L.; Lazarides, A.; Schatz, G. C. *J. Cluster Sci.* **1999**, *10*, 295−317.
(20) Xu, H.; Aizpurua, J.; Käll, M.; Apell, P. *Phys. Rev. E* **2000**, *62*, 4318−24.
(21) Kim, W.; Safonov, V. P.; Shalaev, V. M.; Armstrong, R. L. *Phys. Rev. Lett.* **1999**, *82*, 4811−14.
(22) Mittra, R.; Chan, C. H.; Cwik, T. *Proc. IEEE* **1988**, *76*, 1593−614.
(23) Genov, D. A.; Sarychev, A. K.; Shalaev, V. M. *Phys. Rev. E* **2003**, *67*, 056611.
(24) Goult, R. J. In *Computational Methods in Linear Algebra*; Wiley: New York, 1974.
(25) Xu, H.; Käll, M. *ChemPhysChem* **2003**, *4*, 1001−05.
(26) *Handbook of Optical Constants of Solids*; Palik, E. D., Ed.; Academic Press: New York, 1985.
(27) We note that these calculations are valid only in the relative sense, as the coupled-dipole approximation does not exactly reproduce local electric fields in closely packed arrays of metal nanoparticles. More accurate considerations of retardation effects in closely packed metal nanoparticles deserve further study.
(28) Weitz, D. A.; Garoff, S.; Gramila, T. J. *Opt. Lett.* **1982**, *7*, 168−70.
(29) Nitzan, A.; Brus, L. E. *J. Chem. Phys.* **1981**, *74*, 5321−22. (b) Nitzan, A.; Brus, L. E. *J. Chem. Phys.* **1981**, *75*, 2205−14.
(30) Wokaun, A.; Gordon, J. P.; Liao, P. F. *Phys. Rev. Lett.* **1982**, *48*, 957−60.
(31) Sönnichsen, C.; Franzl, T.; Wilk, T.; von Plessen, G.; Feldmann, J.; Wilson, O.; Mulvaney, P. *Phys. Rev. Lett.* **2002**, *88*, 077402.

NL0343710